NMR analysis of G-protein βγ subunit complexes reveals a dynamic Gα-Gβγ subunit interface and multiple protein recognition modes

Alan V. Smrcka[a,b,c,1], Nessim Kichik[a], Teresa Tarragó[a], Michael Burroughs[b], Min-Sun Park[c,d], Nathan K. Itoga[e], Harry A. Stern[c,d], Barry M. Willardson[e], and Ernest Giralt[a,f,2]

[a]Institute for Research in Biomedicine, Barcelona Science Park, Barcelona, Spain; [b]Department of Pharmacology and Physiology, [c]Department of Biochemistry and Biophysics, and [d]Department of Chemistry, University of Rochester School of Medicine, Rochester, NY 14642; [e]Department of Chemistry and Biochemistry, Brigham Young University, Provo, UT 84602; and [f]Department of Organic Chemistry, University of Barcelona. Martí Franqués, 1. E-08028, Barcelona, Spain

Edited by Melvin I. Simon, California Institute of Technology, Pasadena, CA, and approved November 5, 2009 (received for review August 21, 2009)

G-protein βγ (Gβγ) subunits interact with a wide range of molecular partners including: Gα subunits, effectors, peptides, and small molecule inhibitors. The molecular mechanisms underlying the ability to accommodate this wide range of structurally distinct binding partners are not well understood. To uncover the role of protein flexibility and alterations in protein conformation in molecular recognition by Gβγ, a method for site-specific ^{15}N-labeling of Gβ-Trp residue backbone and indole amines in insect cells was developed. Transverse Relaxation Optimized Spectroscopy-Heteronuclear Single-Quantum Coherence Nuclear Magnetic Resonance (TROSY-HSQC NMR) analysis of ^{15}N-Trp Gβγ identified well-dispersed signals for the individual Trp residue side chain and amide positions. Surprisingly, a wide range of signal intensities was observed in the spectrum, likely representing a range of backbone and side chain mobilities. The signal for GβW99 indole was very intense, suggesting a high level of mobility on the protein surface and molecular dynamics simulations indicate that GβW99 is highly mobile on the nanosecond timescale in comparison with other Gβ tryptophans. Binding of peptides and phosducin dramatically altered the mobility of GβW99 and GβW332 in the binding site and the chemical shifts at sites distant from the direct binding surface in distinct ways. In contrast, binding of $G\alpha_{i1}$-GDP to Gβγ had relatively little effect on the spectrum and, most surprisingly, did not significantly alter Trp mobility at the subunit interface. This suggests the inactive heterotrimer in solution adopts a conformation with an open subunit interface a large percentage of the time. Overall, these data show that Gβγ subunits explore a range of conformations that can be exploited during molecular recognition by diverse binding partners.

Beta gamma subunits | clam shell | Hot Spots | Molecular Recognition | subunit interactions

The Gβγ subunit complex performs a central function transducing signals from G-protein-coupled receptors to changes in cellular physiology through a series of highly regulated protein-protein interactions (1–3). The array of functionally and structurally diverse binding partners both upstream and downstream of Gβγ is not consistent with a simple binding mechanism that relies on well-defined structure or sequence modules (1). Rather, Gβγ appears to have multiple binding modes for interacting with receptors, G-protein α subunits, and downstream effectors (1, 4).

We have proposed that Gβγ subunits have a protein interaction "hot spot" that mediates interactions between Gβγ and downstream signaling molecules and other binding ligands (5, 6). Hot spots are subsets of amino acids in crystallographic protein–protein interfaces that contribute the majority of the interaction energy (7–10). These amino acids tend to be clustered at the center of the interface and present diversity in chemistry that can participate in multiple types of bonding interactions that can be exploited by different binding partners. Additionally, where single protein binding sites interact with multiple diverse ligands, hot spots are flexible and present binding epitopes of variable size and shape, allowing recognition of diverse structures (8). It seems that the Gβγ subunit hot spot must be flexible in order to mediate its multiple diverse binding interactions.

G-protein βγ subunits are potential therapeutic targets based on studies in animal models using protein-based inhibitors of Gβγ functions (11, 12) or genetic deletion of downstream targets of Gβγ signaling (13–15). More recently, small molecule inhibitors of Gβγ subunit signaling have been identified that bind to the Gβγ hot spot and inhibit Gβγ protein–protein interactions (16). These have been used in cellular and animal models to further implicate Gβγ signaling as a potential therapeutic target in pain (17), inflammation (18), and cancer (19). Understanding the flexible nature of this surface is important for developing approaches to target Gβγ with "drug-like" molecules for treatment of disease.

To obtain information about Gβγ flexibility and its importance in ligand binding, we developed an NMR spectroscopy protocol to report on alterations in Gβγ structure. Whereas NMR can provide valuable information about protein structure and dynamics, there are several limitations that must be overcome for success. It is difficult to get informative spectra as the size of the protein increases above 25 kDa because sensitivity decreases as a result of relaxation-dependent line broadening, and the increased number of protons in the macromolecule results in complex spectra with a high degree of spectral overlap (20, 21). To overcome this issue, we prepared Gβγ, selectively labeled with ^{15}N-Trp, to perform two-dimensional ^{1}H-^{15}N-TROSY-HSQC experiments. We have used a similar approach to study ^{15}N-indole-labeled prolyl oligopeptidase (22). Using this method, we examined structural alterations that occurred upon formation of complexes between Gβγ and multiple binding partners. The data reveal that despite binding to similar sets of amino acids on Gβγ, each partner produces unique alterations in the spectra, indicating that different protein conformations are involved in recognition of different binding partners.

Results

Two-Dimensional ^{1}H-^{15}N-TROSY-HSQC Analysis of ^{15}N Tryptophan-Labeled Gβγ. Gβγ was labeled with 2-^{15}N-Trp allowing us to obtain

Author contributions: A.V.S., N.K., T.T., and E.G. designed research; A.V.S., N.K., M.B., and M.P. performed research; A.V.S., M.B., N.K.I., B.M.W., and E.G. contributed new reagents/analytic tools; A.V.S., N.K., T.T., M.P., H.A.S., B.M.W., and E.G. analyzed data; A.V.S., H.A.S., B.M.W., and E.G. wrote the paper.

The authors declare no conflict of interest.

This article is a PNAS Direct Submission.

[1]To whom correspondence may be addressed. E-mail: Alan_Smrcka@urmc.rochester.edu.

[2]To whom correspondence may be addressed. E-mail: ernest.giralt@irbbarcelona.org.

This article contains supporting information online at www.pnas.org/cgi/content/full/0909503107/DCSupplemental.

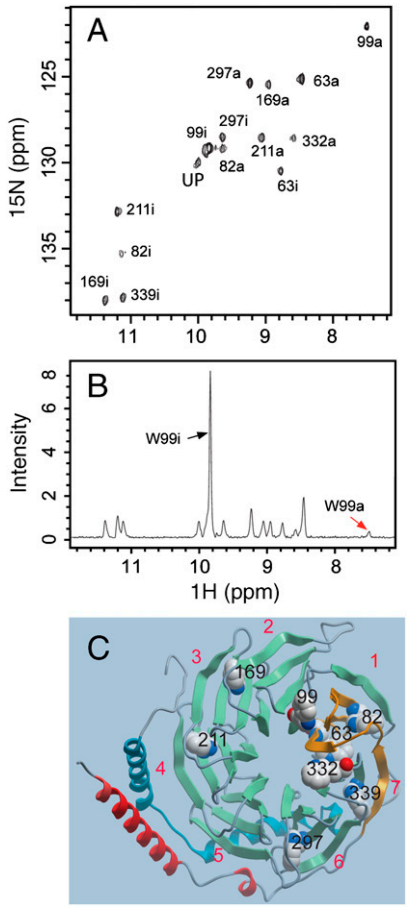

Fig. 1. Two-dimensional ^{1}H-^{15}N-TROSY-HSQC spectrum of G$\beta_1\gamma_2\Delta$C. *A.* Two-dimensional ^{1}H-^{15}N-TROSY-HSQC spectrum of 150 μM ^{15}N-Trp-G$\beta_1\gamma_2\Delta$C acquired for 12 h at 30 °C on a Bruker 800 MHz spectrometer. Assignments were made as discussed in the text and in *Supplemental Material*. The numbering is the amino acid number followed by (*a*) for amide resonances or (*i*) for indole resonances. *UP* is unfolding protein. *B.* ^{1}H-projection of the data in *A*. *Black arrow* indicates the very intense resonance for GβW99i and the *red arrow* indicates an example of a very small signal for GβW99a. *C.* A three-dimensional model of the G$\beta_1\gamma_1$ derived from coordinates 1TBG (23). Red numerals indicate the numbers of the blades of the propeller, according to ref.32, and in black numbering are the Trp residues for which signals are identified in *A*.

two-dimensional ^{1}H-^{15}N-TROSY-HSQC spectra with good dispersion (Fig. 1*A*). For all the peaks, those assigned as the indole or amide are designated with *i* or *a*, respectively. There are eight Trp residues in both core positions of the β propeller of Gβγ, and at critical positions for protein–protein interactions in the Gβγ hot spot (GβW99 and GβW332) (Fig. 1*C*). Of the expected 16 peaks, 14 are observed. The two missing resonances could be either exchange broadened, or overlapping with other signals, as will be discussed, but the overall spectrum was consistent with the expected results. To assign the peaks in the spectrum, we systematically replaced each Trp residue with Phe by site-directed mutagenesis. Two-dimensional ^{1}H-^{15}N-TROSY-HSQC spectra were then obtained for each of the purified Gβγ-Trp mutants and compared with the wt-Gβγ-spectrum to identify missing peaks. Details of the assignments are discussed in *SI Text* and shown in Figs. S1 and S2. One peak was identified as originating from unfolding protein (*UP* in Fig. 1*A*) because its presence was inconsistent and tended to appear and increase as the sample aged. A striking feature of the spectrum was the range of peak intensities, with some low intensity signals (GβW99a, GβW332a and GβW82i) and a very intense signal for GβW99i (Fig. 1*A* and *B*). These differences in intensity likely reflect a range of dynamics of individual Trp side-chain and backbone positions on both fast and intermediate chemical exchange time scales, and indicate significant flexibility of Gβ in the hot spot.

Molecular Dynamics Simulations. We hypothesize that the very intense peak for GβW99i is the result of unusually high mobility on very fast time scale on the protein surface. There are two surface Trp residues, GβW332 and GβW99, but only GβW99i gives this very intense signal. We examined the crystallographic B factors for Trp residues in free Gβγ and only GβW99 had a B factor that was significantly higher than the others (23). To further examine the mobility of GβW99, we performed molecular dynamics simulations. Four dihedral angles were monitored for each Gβ-Trp during 10 independent 8 ns simulations. GβW99 showed significant alteration in these angles on this time scale suggesting that GβW99 has the potential to be highly mobile on the protein surface (Fig. 2 *Left* and Figs. S5 and S7). Interestingly, the backbone ϕ and ψ bond angles in addition to the side chain χ_1 and χ_2 bond angles, showed flexibility and were able to adopt multiple states during these simulations. GβW332, on the other hand, showed little change in dihedral angles (Fig. 2*Right*, Figs. S6 and S8) and is similar to the other Trp residues (Figs. S7 and S8). Also examined was the propensity to form hydrogen bonds that could restrict molecular motion. GβW99 was the only tryptophan that did not participate in hydrogen bonds during the simulations (Table S1). Thus, these simulations support the notion that the strong NMR signal for GβW99 results from a high level of mobility on the nanosecond time scale.

Effects of Peptide Ligand Binding on Resonance Intensities and Chemical Shifts. As an initial experiment to evaluate how Gβγ adapts to binding of ligands and protein partners, we examined alterations in the two-dimensional ^{1}H-^{15}N-TROSY-HSQC spectrum upon binding of two Gβγ binding peptides derived from random peptide phage display (5). These peptides have no sequence homology but bind to the hot spot on Gβγ and competitively inhibit interactions with several downstream targets. We had previously shown that, whereas these peptides bind to an overlapping surface, different subsets of amino acids on Gβ are required for binding (6).

SIGKAFKILGYPDYD (SIGK) is a linear peptide that binds Gβγ with an apparent affinity near 1 μM (5) and the structure of a Gβγ-SIGK cocomplex has been solved (6). In Fig. 3*A* is a comparison of the spectrum of Gβγ alone with Gβγ in the presence of two equivalents of SIGK. The most striking alteration is the dramatic decrease in intensity and change in chemical shift for the GβW99i signal. This result is consistent with the three-dimensional structure of the SIGK-Gβγ cocomplex where SIGK binding would restrict the motion of GβW99 (6).

Also observed were significant increases in the intensity for the GβW99a, a shift in position of the GβW332a resonance and appearance of a new signal (Fig. 3*A*) corresponding to one of

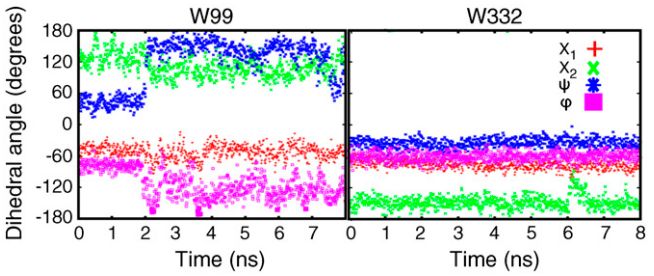

Fig. 2. Molecular dynamics simulations for Gβγ-Trp resonances. Example 8-ns trajectories for ϕ, ψ, χ1, and χ2 bond angles for GβW99 (*Left*) and GβW332 (*Right*). Calculations were performed 10 times with different starting points for each Trp residue as described in *Methods*.

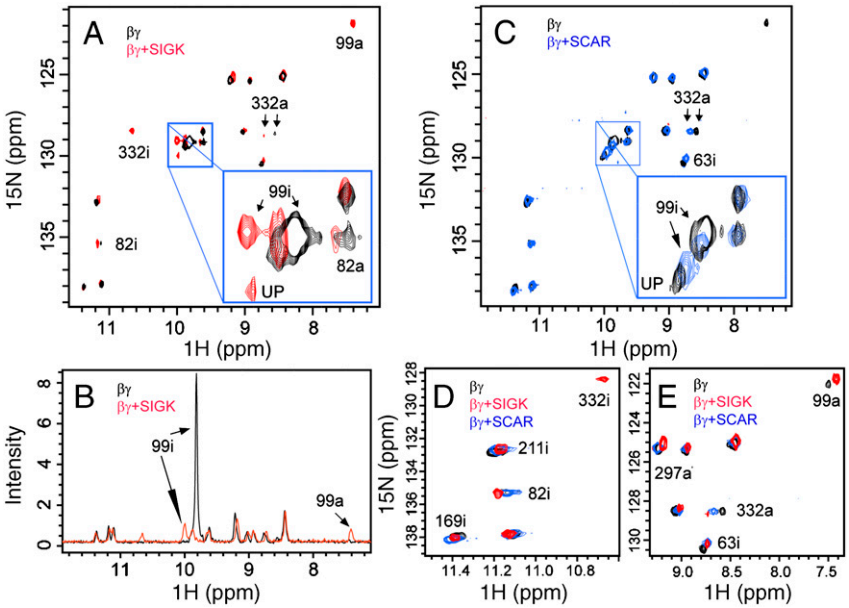

Fig. 3. Peptide ligand effects on G$\beta_1\gamma_2\Delta$C ^{1}H-^{15}N-TROSY-HSQC spectrum. *A.* Comparison of HSQC spectrum of ^{15}N-Trp-G$\beta_1\gamma_2\Delta$C (150 μM) in the absence (*Black*) and presence (*Red*) of 300 μM SIGK: SIGKAFKILGYPDYD. *B.* ^{1}H projection of the ^{1}H-^{15}N-TROSY-HSQC spectra from *A*. *C.* Comparison of ^{1}H-^{15}N-TROSY-HSQC spectrum of ^{15}N-Trp-G$\beta_1\gamma_2\Delta$C (150 μM) in the absence (*Black*) and presence (*Blue*) of 300 μM SCAR: SCARFFGTPGCT. *D.* Comparison of the downfield region of the ^{1}H-^{15}N-TROSY-HSQC spectra from Gβγ alone (*Black*) Gβγ with SIGK (*Red*) and Gβγ with SCAR (*Blue*). *E.* Comparison of the upfield region of the ^{1}H-^{15}N-TROSY-HSQC spectra from Gβγ alone (*Black*) Gβγ with SIGK (*Red*) and Gβγ with SCAR (*Blue*).

the missing peaks in the unbound spectrum that can be attributed to GβW332i (Fig. S1*F*). GβW332 also directly contacts SIGK in the three-dimensional structure (6). The most likely explanation for these observations is that in the ligand-free state, the signal for GβW332i is unobservable, and the GβW99a signal is very weak due to line broadening resulting from chemical exchange between different conformations on an intermediate time scale. Direct binding of SIGK preferentially stabilizes one of these conformations, resulting in an increase in observable NMR signal. In addition to changes that occur due to direct interactions between the peptide and the hot spot, a number of alterations occur at amino acids at some distance from the peptide binding site including: GβW297a, GβW82a, GβW211a, GβW82i, GβW63i and GβW339i. Most of these changes are not large but they are significant and indicate that binding of ligands to the hot spot can transmit conformational information throughout the Gβ subunit structure.

We also examined alterations in the spectrum that occurred with a second peptide SCARFFGTPGCT (SCAR). This peptide is very different in sequence from SIGK and is constrained in a cyclic conformation by an internal disulfide bond, and is a competitive inhibitor of some Gβγ-effector interactions with an apparent affinity for Gβγ similar to SIGK (6). Like SIGK, SCAR binding suppresses the intense GβW99i resonance but, in the case of SCAR, there was no effect on GβW99a (Fig. 3*C*). There was also a shift in GβW332a resonance but to a different position than SIGK and no increase in GβW332i resonance was observed. At positions distant from the binding sites for the peptides, there are additional similarities and differences between the spectral changes caused by the binding of the two peptides (Fig. 3*D* and *E*).

G-Protein α Subunit Binding. G-protein α subunits bind to Gβγ subunits with 1–10 nM affinity (24) and also interact with the Gβγ hot spot. The switch II region of Gα subunit has high structural homology with SIGK and interacts with all of the same amino acids in the hot spot (Fig. 4*A* and Table S2). Gα has additional contacts outside of the hot spot, as well (Fig. 4*A* and Table S2). To assess the effects of Gα on Gβγ conformation, we assembled ^{15}N-Trp-Gβγ subunit with unlabeled myristoylated-Gα_{i1}-GDP (mGα_{i1}-GDP) subunits in a 1 : 1.2 molar ratio and performed ^{1}H-^{15}N-TROSY-HSQC analysis. Assembly with mGα_{i1}-GDP subunits resulted in remarkably little change in the ^{15}N-Trp-Gβγ spectrum (Fig. 4*B*). Particularly striking was the lack of effect of mGα_{i1}-GDP binding on the apparent mobility of GβW99i. Whereas the binding of SIGK peptide resulted in complete suppression of the GβW99i resonance, assembly with mGα_{i1}-GDP resulted in only a partial 30–50% suppression of this signal (Fig. 4*C*). This suggests that GβW99 retains a high level of mobility in the assembled inactive heterotrimer. There is also a loss of the GβW99a signal with mGα_{i1}-GDP binding but this is difficult to interpret because the signal is very weak in the absence of mGα_{i1}-GDP and the noise increases significantly upon formation of the large Gαβγ complex, which possibly leads to loss of low intensity peaks. Upon addition of the G-protein activator, aluminum fluoride, the intensity of GβW99i is restored to the intensity observed in the unbound state. The lack of increase in intensity of other signals suggests that Gα remains bound to Gβγ because the overall signal should increase due to the decrease in molecular weight upon Gα dissociation (Fig. S4).

Several lines of evidence suggest that mGα_{i1}-GDP was properly assembled with Gβγ. Upon assembly with mGα_{i1}-GDP, a quality spectrum was no longer achievable on the 600 MHz spectrometer and acquisition of the spectrum required analysis on the 800 MHz spectrometer that is indicative of a loss of sensitivity due to relaxation-dependent line broadening that occurred upon formation of the higher molecular weight species. Dynamic light scattering analysis of the NMR sample indicated an approximate doubling in the molecular weight upon assembly of Gβγ with mGα_{i1}-GDP. Only one molecular weight species corresponding to assembled heterotrimer was present indicating little aggregated protein, free Gα, or Gβγ in the sample (Fig. S3).

Phosducin Binding. Phosducin is a protein found in the retina that binds Gβγ and can inhibit its activity. It has been cocrystallized with Gβγ and local conformational alterations in Gβγ are observed in the complex (25, 26). To compare the extent and pattern of structural alterations in solution with another Gβγ binding

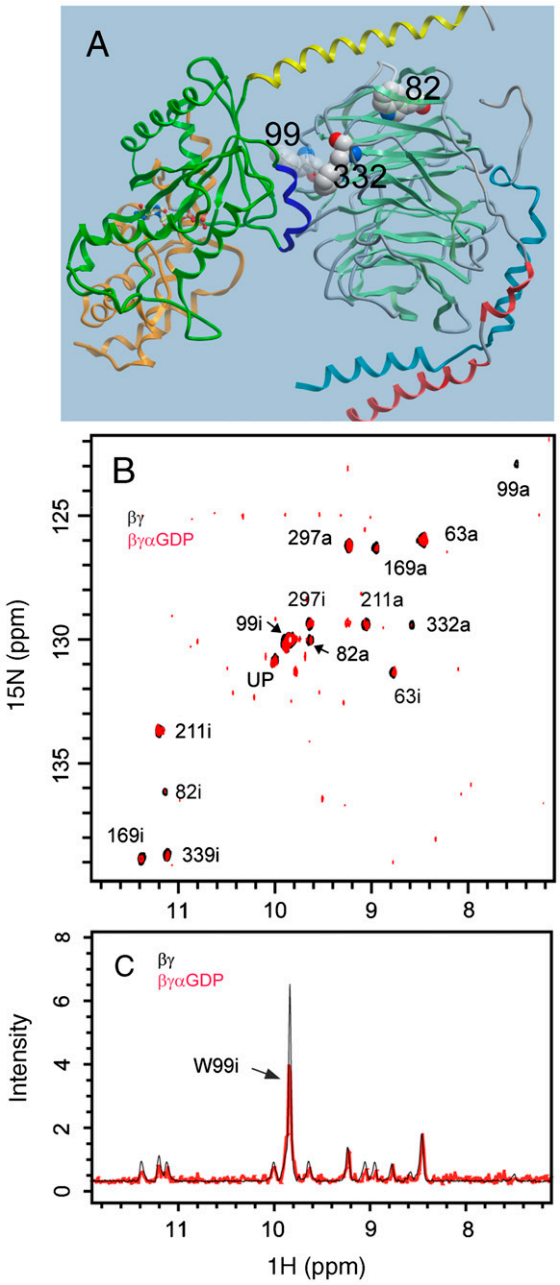

Fig. 4. Gα subunit effects on $G\beta_1\gamma_2\Delta C$ ^1H-^{15}N-TROSY-HSQC spectrum. *A.* Model of the three-dimensional structure of the $G\alpha_{i1}G\beta_1\gamma_2$ heterotrimer from coordinates 1GP2. Key Gβγ subunit Trp residues are numbered in *Black*. The *Dark Blue* helix is the switch II region of Gα and the *yellow* helix is the N-terminal helix of $G\alpha_i$. *B.* Overlay of the ^1H-^{15}N-TROSY-HSQC spectra of the 1.2:1 complex of Gα-^{15}N-Trp-$G\beta_1\gamma_2\Delta C$ (*Red*) to ^{15}N-Trp-$G\beta_1\gamma_2\Delta C$ alone (*Black*). Data were collected for 12 h for ^{15}N-Trp-$G\beta_1\gamma_2\Delta C$ alone and 24 h for the complex by using an 800 MHz spectrometer for both. *C.* ^1H projection of the data in *B*.

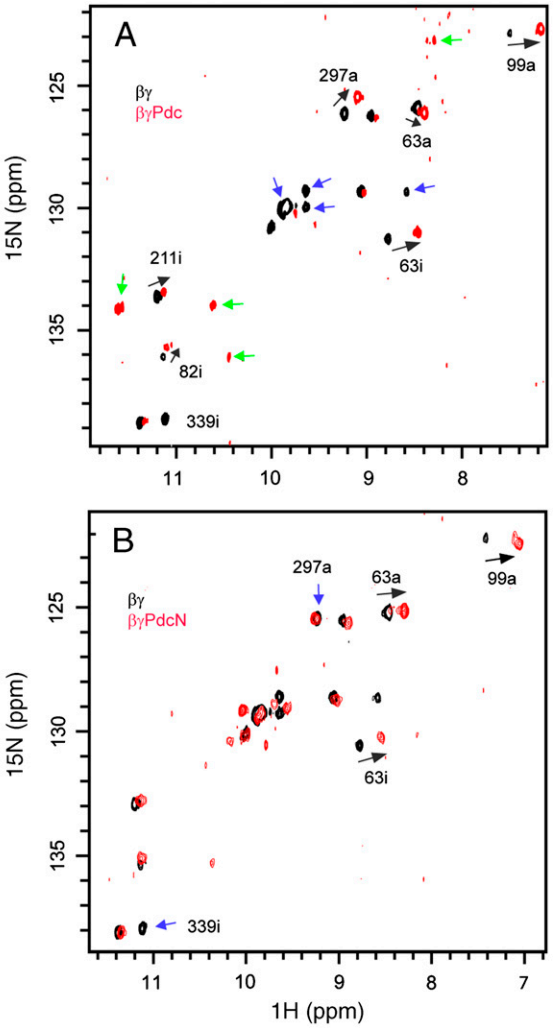

Fig. 5. Phosducin binding to Gβγ. *A.* Comparison of ^1H-^{15}N-TROSY-HSQC spectrum of free Gβγ (*Black*) and Gβγ-phosducin complex (*Red*). *Black arrows* indicate shifts of resonance position in the complex, *Blue arrows* indicate resonances that disappear in the complex, and *Green arrows* indicate resonances that appear in the complex but cannot be assigned. *B.* Comparison of ^1H-^{15}N-TROSY-HSQC spectrum of free Gβγ (*Black*) and Gβγ -phosducin N terminus 1–107 complex (*Red*). *Black arrows* indicate changes that are similar to the Gβγ full-length phosducin complex and *Blue arrows* indicate differences from the full-length complex.

partner, a complex between unlabeled phosducin (Pdc) and ^{15}N-Trp Gβγ was analyzed by two-dimensional ^1H-^{15}N-TROSY-HSQC (Fig. 5*A*). The results are in striking contrast to those observed in the complex with $G\alpha_{i1}$. Phosducin binding results in significant alterations in peak intensities and/or chemical shifts for virtually all the Trp residues. GβW99 and GβW332 in the hot spot directly contact the N terminus of phosducin and their signals are strongly altered. The resonance for GβW339i is also altered and, whereas GβW339 does not directly interact with phosducin, it is positioned to report on the local conformational changes observed in crystal structures of the complex (25, 26) that open the cavity between blades six and seven (see Fig. 1*C*) upon Pdc-binding. More surprising are changes observed for Trp residues distant from the binding site of phosducin on Gβγ. These other Trp residues are structural elements of the blades of Gβ and the changes in chemical shift report overall structural changes in the propeller in solution that are not obvious from the three-dimensional crystal structures.

Phosducin consists of two discreet domains that interact with the Gβ propeller, an N-terminal region that interacts with the hot spot and a C-terminal region that interacts with blades six and seven (see Fig. 1*C*). To more specifically determine the role of binding at the hot spot in the observed conformational alterations, a protein consisting of amino acids 1–107 from phosducin (PdcN) was purified and complexed with ^{15}N-Trp-Gβγ. The two-dimensional ^1H-^{15}N-TROSY-HSQC spectrum (Fig. 5*B*) shows many, but not all, of the alterations observed with full-length phosducin. Thus binding of the N-terminal domain of phosducin is sufficient to alter the global conformation of Gβ but the

C terminus can modify the nature of these changes to some degree.

Discussion

The two-dimensional ^{1}H-^{15}N-TROSY-HSQC spectrum for Gβγ reveals a striking range of intensities of NMR signals in the spectrum. We propose that this represents a range of dynamic properties of each of these amino acids on Gβ on different NMR time scales. Evidence that the diversity of peak intensities represent conformational exchange on different time scales are: (*i*) Molecular dynamics simulations that show that GβW99 has the capacity to be uniquely mobile on a nanosecond timescale. (*ii*) GβW99i peak intensity is greatly diminished by SIGK binding consistent with the crystal structure showing that GβW99i-side chain mobility would be severely restricted upon peptide binding (6). (*iii*) The low intensity signals of both the GβW99a and GβW332i increase upon SIGK binding to a level similar to the mean for the remaining amino acids. This can be best explained by chemical exchange between different conformations on an intermediate time scale (μsec-msec) in the unbound protein, with SIGK binding selecting and stabilizing a single conformation. This hypothesis is supported by x-ray diffraction data showing direct interactions of SIGK with GβW332 that would alter the dynamic properties of this amino acid.

A quantitative approach to measuring individual Trp side chain and backbone dynamics would require rigorous chemical relaxation experiments (27–29). Several factors limit this approach for this study, including long times (12 h) for two-dimensional ^{1}H-^{15}N-TROSY-HSQC data acquisition, and uncertain protein stability for collecting multiple relaxation spectra. Additionally, the intensities of some of the signals are extremely low or not observable, making it difficult to follow their evolution over the course of the relaxation experiment. Qualitatively, however, the data supports the conclusion that many of the Trp residues in unbound Gβγ undergo chemical exchange between different conformations on different time scales. We only observe Trp residues in these spectra but it is likely that other amino acids in the hot spot are dynamic, as well. This range of dynamics supports the hypothesis that the hot spot of Gβ subunits explores a range of conformations in the ligand-free state that present a range of structures that can be selected for by a particular binding partner. This concept could be important for explaining the ability of Gβγ to bind to multiple protein and small-molecule ligands.

Of particular interest is the contrast in Gβγ-conformational states bound by Gα, SIGK, and phosducin binding to Gβγ. Of these proteins, m$G\alpha_{i1}$-GDP has the highest affinity for Gβγ with a Kd of 1–10 nM (24), whereas phosducin and SIGK have Kd´s of 50 nM (30) and 1 μM (31), respectively. The studies presented here were performed with Gβγ subunits missing the geranyl–geranyl lipid that is important for high-affinity interactions between Gβγ and various protein binding partners including: Gα and phosducin. However; at high concentrations of Gβγ, such as in the conditions of our NMR experiments (150 μM), Gβγ binds to all these partners (32–34). SIGK is a structural mimic of Gα switch II, interacts with the same amino acids as Gα switch II, and has clear effects on the mobility and chemical shifts of Trp residues inside and outside the hot spot. Striking differences in the NMR spectrum are also observed either in Pdc or PdcN complexes compared to that of free-Gβγ. Thus, it is remarkable that very little difference is observed in m$G\alpha_{i1}$-GDP subunit bound spectrum of Gβγ compared to free-Gβγ. Most surprising is the level of apparent mobility that is maintained for both of the Trp residues in the hot spot, particularly GβW99i. This would not be possible if the solution conformation of the heterotrimer was the same as that reported in the crystal structures with GβW99i involved in hydrogen bond and van der Waals interactions with Gα amino acids (32–34). These data strongly suggest that the inactive heterotrimer is in an open conformation exposing the Gβγ hot spot and Gα switch II interface a large percentage of the time allowing for increased mobility of amino acids at this interface.

In an open conformation, the inactive heterotrimer could interact with effectors or other molecules through either Gβγ, Gα,or both surfaces in the absence of nucleotide exchange. Nucleotide exchange could increase the availability of these surfaces or alter the relative conformations of these surfaces to lead to effector activation. The opening of this surface also provides a potential mechanism for nucleotide exchange-independent G-protein activation such as observed for some Activators of G protein Signaling (AGS) proteins (35–37) that seem to promote G-protein subunit dissociation through interaction with these surfaces in the inactive heterotrimer.

A general view in the field is that Gβγ subunits do not undergo significant conformational changes primarily based on observations comparing the free-Gβγ structure with Gβγ cocomplexes. In the studies presented here, SIGK, SCAR, Gα subunits, and phosducin binding yield distinct changes in chemical shift at sites within and outside the direct binding surface. For SIGK and SCAR, the major changes in chemical shift and dynamics are observed for GβW99i, GβW332i, and GβW99a; all directly in the peptide binding site. These alterations may reflect local alterations in conformation, but the additional, albeit subtle, changes in chemical shift that occur outside the peptide binding site indicate more global structural changes. For Gα subunits, any changes outside the binding site were difficult to observe. In contrast, are the dramatic changes that occur throughout the protein upon phosducin binding despite the 10-fold lower affinity of phosducin than Gα for Gβγ. The data supports the idea that the conformational change believed to bury the prenyl group in a groove between β-propeller blades six and seven may be more global than originally proposed from the crystal structures (25, 26). The fact that similar structural changes in Gβγ were observed with full length Pdc and its N-terminal domain is consistent with biochemical studies showing that they both caused dissociation of Gβγ from membranes despite the fact that only the C-terminal domain sterically interferes with membrane binding (38). This finding led to the prediction that the N-terminal domain could allosterically induce the conformation with the prenyl group buried.

Together these data strongly support the hypothesis that Gβγ subunits accommodate different binding partners through structurally distinct conformations. To date, there are crystal structures of cocomplexes between Gβγ and phosducin (25, 26), Gβγ and Gα subunits (32, 35), Gβγ and G-protein-coupled receptor kinase 2 (39), and Gβγ and SIGK (6) or parathyroid hormone receptor (40) peptides. There are close to 50 different binding partners for Gβγ and our data suggest that there are changes in conformation of Gβγ that occur in solution that are not readily observed or interpretable from crystallographic structures. Thus it seems very likely that there are a wide range of structural changes that can occur on Gβγ that depend on the binding partner, and these conformational changes could be important not only for molecular recognition but for modulation of Gβγ signaling functions.

Materials and Methods

Expression and Purification of ^{15}N-Trp Gβγ. Gβ_1 (or Gβ_1-Trp mutants) and 6His-tagged γ_2 truncated after F67 to remove the site of isoprenylation and the distal amino acids in the Cysteine, aliphatic, aliphatic, X amino acids (CAAX) box were expressed in High 5 insect cells grown in custom media (Bioexpress 2000; Cambridge Isotope Laboratories) supplemented with unlabeled amino acids, except for Trp isotopically labeled with ^{15}N at the α-amine and ε-indole positions (Cambridge Isotope Laboratories). Protein was purified, as has been described previously, and as in *SI Materials and Methods*. The yield is 1–3 mg of pure ^{15}N labeled ^{15}N-6His-$\beta_1\gamma_2\Delta$C. All protein concentrations were estimated with a Bradford protein assay.

NMR Analysis of ^{15}N Gβγ. 160–200 μl of sample in NMR buffer: 20 mM $NaHPO_4$, pH 7.0, 100 mM NaCl, and 10% D_2O was introduced into a 3 mm NMR tube. The analysis used 600 and 800 MHz Bruker Digital Avance NMR instruments fitted with triple-resonance z-axis gradient cryoprobes. The 600 MHz instrument was used for most of the experiments, although the 800 MHz instrument was used where indicated. Measurements were conducted by using a ^{1}H-^{15}N-TROSY-HSQC pulse sequence and data were collected for 8–12 h (unless otherwise indicated) at 30 °C. Data were processed by using Topspin 2.0. To normalize for alterations in overall spectral intensities between samples and experiments, spectra were adjusted to the relatively fixed signal of GβW63a. Thus discussions of spectral intensities refer to relative intensities within a given spectrum. To assess sample integrity, 1-D proton NMR spectra were taken before and after each 2-D experiment. No significant changes were observed in the protein spectra indicating a lack of aggregation or protein loss over the course of the measurements.

Formation of Gβγ Complexes. For formation of $G\beta_1\gamma_2$-myristoylated-$G\alpha_{i1}$GDP complexes and 32.6 nmoles of $G\beta_1\gamma_2\Delta C$ was mixed with 40 nmoles of Gα subunits (0.9 mol/mol GTPγS binding) in 2.5 ml buffer *A*: NMR buffer containing 25 μM GDP and 200 μM Dithiothreitol (DTT). The mixture was gel filtered into 3.5 ml of buffer *A*, followed by centrifugal concentration to 200 μl. A similar procedure was used to form phosducin complexes except GDP was not included. For formation of peptide complexes, small aliquots of 10 mM SIGK or SCAR dissolved in NMR buffer were directly added to the concentrated Gβγ NMR sample. No DTT was added to these complexes but a small amount of 2-mercaptoethanol was present that was residual from the Gβγ preparation.

Simulations. All simulations were performed with the AMBER9 software package by using the parm99 parameter set. The initial structure of the G-protein was based on the crystallographic structure of Gβγ complex with the SIGK peptide ligand (Protein Data Bank (PDB) code 1XHM). The SIGK ligand was removed from the original complex. To create a set of initial conformations, 1 ns simulations of the receptor or bound complex were performed by using the Generalized Born implicit solvent model and Langevin dynamics at 300 K. Configurations from these simulations were saved and assigned to nine clusters on the basis of root-mean-square deviation. For each cluster, the configuration closest to the cluster center was used as the starting structure for an 8-ns molecular dynamics simulation performed with explicit solvent. Simulations by using the crystal structure as an initial configuration were also performed, for a total of ten independent 8-ns simulations. See *Supporting Information Materials and Methods* for details.

ACKNOWLEDGEMENTS. This work was supported by National Institutes of Health Grant GM081772 (to A.V.S.); MCYT-FEDER (Bio2008-00799); and the *Generalitat de Catalunya* (X.R.B. and *Grup Consolidat*) (E.G.).

1. Smrcka AV (2008) G protein βγ subunits: central mediators of G protein-coupled receptor signaling. *Cell Mol Life Sci*, 65:2191–2214.
2. Dupre DJ, Robitaille M, Rebois RV, Hebert TE (2009) The role of Gβγ subunits in the organization, assembly, and function of GPCR signaling complexes. *Annu Rev Pharmacol Toxicol*, 49:31–56.
3. Oldham WM, Hamm E (2006) Structural basis of function in heterotrimeric G proteins. *Q Rev Biophys*, 39:117–166.
4. Ford CE, et al. (1998) Molecular basis for interactions of G protein βγ subunits with effectors. *Science*, 280:1271–1274.
5. Scott JK, et al. (2001) Evidence that a protein-protein interaction "hot spot" on heterotrimeric G protein βγ subunits is used for recognition of a subclass of effectors. *EMBO J*, 20:767–776.
6. Davis T, Bonacci TM, Sprang SR, Smrcka AV (2005) Structural Definition of a Preferred Protein Interaction Site in the G protein β1γ2 heterodimer. *Biochemistry*, 44:10593–10604.
7. Atwell S, Ultsch M, Devos AM, Wells JA (1997) Structural plasticity in a remodeled protein-protein interface. *Science*, 278:1125–1128.
8. Delano WL, Ultsch MH, de Vos AM, Wells JA (2000) Convergent solutions to binding at a protein-protein interface. *Science*, 287:1279–1283.
9. Wells JA, Devos AM (1996) Hematopoietic receptor complexes. *Annu Rev Biochem*, 65:609–634.
10. Gordo SI, Giralt E (2009) Knitting and untying the protein network: modulation of protein ensembles as a therapeutic strategy. *Protein Sci*, 18:481–493.
11. Bookout AL, et al. (2003) Targeting Gβγ Signaling to inhibit prostate tumor formation and growth. *J Biol Chem*, 278:37569–37573.
12. Koch WJ, et al. (1995) Cardiac function in mice overexpressing the β-adrenergic receptor kinase or a βARK inhibitor. *Science*, 268:1350–1353.
13. Xie W, et al. (1999) Genetic alteration of phospholipase Cβ3 expression modulates behavioral and cellular responses to μ opioids. *Proc Natl Acad Sci USA*, 96:10385–10390.
14. Li Z, et al. (2000) Roles of PLC-2 and -3 and PI3K in Chemoattractant-Mediated Signal Transduction. *Science*, 287:1046–1049.
15. Hirsch E, et al. (2000) Central role for G protein-coupled phosphoinositide 3-Kinase γ in inflammation. *Science*, 287:1049–1053.
16. Bonacci TM, et al. (2006) Differential targeting of Gβγ-subunit signaling with small molecules. *Science*, 312:443–446.
17. Mathews JL, Smrcka AV, Bidlack JM (2008) A novel Gβγ-subunit inhibitor selectively modulates μ-opioid-dependent antinociception and attenuates acute morphine-induced antinociceptive yolerance and dependence. *J Neurosci*, 28:12183–12189.
18. Lehmann DM, Seneviratne AMPB, Smrcka AV (2008) Small molecule disruption of G protein βγ subunit signaling inhibits neutrophil chemotaxis and inflammation. *Mol Pharmacol*, 73:410–418.
19. Qin J, et al. (2009) Upregulation of PIP3-dependent Rac exchanger 1 (P-Rex1) promotes prostate cancer metastasis. *Oncogene*, 28:1853–1863.
20. Pellecchia M, et al. (2008) Perspectives on NMR in drug discovery: A technique comes of age. *Nat Rev Drug Discovery*, 7:738–745.
21. Tugarinov V, Hwang PM, Kay LE (2004) Nuclear magnetic resonance spectroscopy of high-molecular-weight proteins. *Annu Rev Biochem*, 73:107–146.
22. Tarrago T, et al. (2009) A cost-effective labeling strategy for the NMR study of large proteins: Selective ^{15}N-labeling of the tryptophan side chains of prolyl oligopeptidase. *ChemBioChem*, 10:2736–2739.
23. Sondek J, et al. (1996) Crystal structure of a G-protein βγ dimer at 2.1 Å resolution. *Nature*, 379:369–374.
24. Sarvazyan NA, Remmers AE, Neubig RR (1998) Determinants of Giα and βγ binding: Measuring high affinity interactions in a lipid environment using flow cytometry. *J Biol Chem*, 273:7934–7940.
25. Gaudet R, Bohm A, Sigler PB (1996) Crystal structure at 2.4 angstroms resolution of the complex of transducin βγ and its regulator, phosducin. *Cell*, 87:577–588.
26. Loew A, Ho YK, Blundell T, Bax B (1998) Phosducin induces a structural change in transducin βγ. *Structure*, 6:1007–1019.
27. Palmer AG, III (2001) NMR probes of molecular dynamics: Overview and comparison with other techniques. *Annu Rev Biophys Biomol Struct*, 30:129–155.
28. Mittermaier A, Kay LE (2006) New tools provide new insights in NMR studies of protein dynamics. *Science*, 312:224–228.
29. Boehr DD, Dyson HJ, Wright PE (2006) An NMR perspective on enzyme dynamics. *Chem Rev*, 106:3055–3079.
30. Savage JR, et al. (2000) Functional roles of the two domains of phosducin and phosducin-like protein. *J Bio Chem*, 275:30399–30407.
31. Ghosh M, Peterson YK, Lanier SM, Smrcka AV (2003) Receptor and nucleotide exchange independent mechanisms for promoting G protein subunit dissociation. *J Biolchem*, 273:34747–34750.
32. Wall MA, et al. (1995) The structure of the G protein heterotrimer $Gi\alpha_1\beta_1\gamma_2$. *Cell*, 83:1047–1058.
33. Sprang SR (1997) G protein mechanisms: Insights from structural analysis. *Annu Rev Biochem*, 66:639–678.
34. Lambright DG, et al. (1996) The 2.0 Å crystal structure of a heterotrimeric G protein. *Nature*, 379:311–319.
35. Blumer JB, Cismowski MJ, Sato M, Lanier SM (2005) AGS proteins: receptor-independent activators of G-protein signaling. *Trends Pharmacol Sci*, 26:470–476.
36. Blumer JB, Smrcka AV, Lanier SM (2007) Mechanistic pathways and biological roles for receptor-independent activators of G-protein signaling. *Pharmacol Ther*, 113:488–506.
37. Yuan C, Sato M, Lanier SM, Smrcka AV (2007) Signaling by a non-dissociated complex of G protein βγ and α subunits stimulated by a receptor-independent activator of G protein signaling, AGS8. *J Bio Chem* , 282:19938–19947.
38. Lukov GL, et al. (2004) Role of the isoprenyl pocket of the G protein βγ subunit complex in the binding of phosducin and phosducin-like protein. *Biochemistry*, 43:5651–5660.
39. Lodowski DT, et al. (2003) Keeping G proteins at bay: A complex between G protein-coupled receptor kinase 2 and Gβγ. *Science*, 300:1256–1262.
40. Johnston CA, Kimple AJ, Giguere PM, Siderovski DP (2008) Structure of the parathyroid hormone receptor C terminus bound to the G-protein dimer $G\beta_1\gamma_2$. *Structure*, 16:1086–1094.